

Image quality assessment of ultra low-dose chest CT using sinogram-affirmed iterative reconstruction

So Won Lee · Yookyung Kim · Sung Shine Shim ·
Jeong Kyong Lee · Seok Jeong Lee · Yon Ju Ryu ·
Jung Hyun Chang

Received: 22 October 2013 / Revised: 16 December 2013 / Accepted: 17 December 2013 / Published online: 18 January 2014
© European Society of Radiology 2014

Abstract

Objectives To assess the image quality of ultra-low-dose computed tomography (ULDCT) using sinogram-affirmed iterative reconstruction (SAFIRE) compared to reduced dose CT (RDCT).

Methods Eighty-one consecutive patients underwent non-enhanced ULDCT using 80 kVp and 30 mAs and contrast-enhanced RDCT using automated tube potential selection and tube current modulation. CT images were reconstructed with SAFIRE. Image noise and subjective image quality of normal structures and various pulmonary lesions were assessed.

Results The mean effective doses were 0.29 ± 0.03 and 2.88 ± 1.11 mSv for ULDCT and RDCT, respectively. ULDCT had significantly higher noise ($p < 0.001$). Image quality of five normal structures was diagnostic in 91.1 % of ULDCT and 100 % of RDCT. With ULDCT, the frequencies of non-diagnostic image quality were 2.0 (1/50), 4.6 (13/280), 25.5 (14/55), and 40.0 (8/20)% for BMIs of <20 , 20–25, 25–30, and >30 . In the assessment of pulmonary lesions, non-diagnostic image quality was observed for 11.2 % of all lesions, 60.9 % of decreased attenuation (significantly more frequent for upper lung lesions), and 23.5 % of ground-glass nodules.

Conclusion ULDCT generates diagnostic images in patients with a BMI ≤ 25 , but is of limited use for lesions with

decreased attenuation, ground-glass nodules, or those located in the upper lobe.

Key Points

- Iterative reconstruction enables ultra-low-dose CT (ULDCT) with very low radiation doses.
- Image quality of ULDCT depends on the patient body mass index (BMI).
- Selection of kVp and mAs depends on both BMI and lesion type.
- Diagnosis of pulmonary emphysema or ground-glass nodules requires higher radiation doses.

Keywords Computed tomography · Iterative reconstruction · Radiation dose reduction

Introduction

The introduction of helical and multi-detector row CT has greatly increased the clinical indications and diagnostic accuracy of CT. As a result, the total numbers of CT examinations have increased, raising concern among radiologists regarding radiation exposure from CT among the population, which must be weighed against diagnostic image quality.

Various imaging techniques have been developed to reduce the radiation dose, including tube current modulation techniques [1,2], lower tube voltage techniques [3], noise-reduction filters [4], and iterative reconstruction algorithms [5–7]. Among these methods, the iterative reconstruction technique is a recently introduced method that offers an alternative to the conventional reconstruction by filtered back-projection (FBP). This method repeatedly eliminates image noise and artefacts arising from the low radiation dose during the iterative reconstruction process, substantially reducing the radiation dose to produce diagnostic image quality.

S. W. Lee · Y. Kim · S. S. Shim · J. K. Lee
Department of Radiology, School of Medicine, Ewha Womans University, Seoul, South Korea

S. J. Lee · Y. J. Ryu · J. H. Chang
Division of Pulmonology in the Department of Internal Medicine, School of Medicine, Ewha Womans University, Seoul, South Korea

Y. Kim (✉)
Department of Radiology, Ewha Womans University Mokdong Hospital, 1071, Anyangcheon-ro Yangcheon-gu Seoul 158-710, Korea
e-mail: yookkim@ewha.ac.kr

Sinogram-affirmed iterative reconstruction (SAFIRE) is a new iterative reconstruction algorithm using a noise modeling technique supported by raw data. To our knowledge, only a single preliminary report of ULDCT using SAFIRE [6] has been published; further investigation is needed for its clinical application.

The purpose of our study was to assess both the objective and subjective image quality of ULDCT obtained using SAFIRE at a tube potential of 80 kVp. We compared the image quality of ULDCT with RDCT, and evaluated the relationship between image quality and body mass index (BMI) and the characteristics and location of various pulmonary lesions.

Materials and methods

Patients

This retrospective study was approved by the institutional review board, and written informed consent was waived. Images were obtained from 81 consecutive patients who underwent chest CT scans that included non-contrast enhanced ULDCT, followed by a post-contrast-enhanced RDCT. Imaging took place from December 2012 to January 2013, and all patient CTs were analysed retrospectively. The CT protocol was designed for our hospital after the introduction of an automated attenuation-based tube potential selection and iterative reconstruction algorithm enabling the reduction of total radiation dose in two CT examinations. This protocol is helpful in our country, which has a high incidence of tuberculosis, and is suitable for patients with intra- or extrathoracic malignancy or pulmonary nodules of unknown aetiology in whom the detection of calcification or high attenuation in lymph nodes or lung nodules on a non-enhanced CT is helpful for the differentiation between benign and malignant lesions.

A total of 29 men and 52 women were enrolled, with a mean age of 57.2 ± 12.8 years [mean \pm standard deviation (SD); range, 18–85 years]. The body mass index (BMI) of each patient was calculated from the data available in the medical records; the average BMI of patients was 23.6 ± 3.8 kg/m² (range, 18.8–33.1 kg/m²). Clinical indications for chest CT included a follow-up study of primary or metastatic lung malignancy, a solitary pulmonary nodule on the radiograph, or fluorine-18-fluorodeoxyglucose positron emission tomography (FDG-PET) abnormality. Clinical diagnoses were lung cancer ($n=18$), breast cancer ($n=24$), extrathoracic malignancy ($n=18$), tuberculosis ($n=12$), and others ($n=8$). Image noise, overall image quality of normal structures, and subjective image quality for various pulmonary lesions were evaluated in all patients.

CT examination

All CT images were obtained in the supine position using a dual-source multidetector row scanner (SOMATOM Definition Flash; Siemens Medical Solutions, Forchheim, Germany). Ultra-low-dose CT was performed at 80 kVp, 30 mAs (effective), $2 \times 64 \times 0.6$ -mm collimation, a pitch of 1.2, and a gantry rotation time of 0.5 s before intravenous injection of contrast material. The subsequent RDCT was acquired after contrast injection. All parameters remained unchanged, except that the tube potential was determined by an automated attenuation-based tube potential selection (CAREkV; Siemens Medical Solutions) and on-line dose modulation (Care DOSE 4D; Siemens Medical Solutions) enabled. CT was performed using 80kVp/ 273 ref mAs in 5 patients, 100 kVp/ 121 ref mAs in 66 patients, and 120 kVp/90 ref mAs in 10 patients. The CT image was obtained 40 s after intravenous injection of 100 ml of a nonionic contrast agent (iohexol, Bonorex 350; CMS, Seoul, Korea) at a rate of 2.3 ml/s via automatic dual-head power injection. The mean time interval between ULDCT and RDCT was 63.1 ± 6.4 s.

Data reconstruction

Both ULDCT and RDCT were reconstructed by sinogram-affirmed iterative reconstruction (SAFIRE, Siemens Healthcare, Forchheim, Germany), using a high spatial resolution kernel (I70) and two iterations for lung window images and a soft resolution kernel (I40) and two iterations for mediastinal window images, respectively. All images were reconstructed in a transverse orientation at a slice thickness of 2 mm and an increment of 2 mm, and transferred to a picture-archiving and communication system (PACS) (INFINITT; Infinitt Healthcare, Seoul, Korea).

Image analysis

Image analyses were performed using a PACS viewer (INFINITT PiViewSTAR; Infinitt Healthcare) with two 21-inch black and white monitors (resolution, $2,048 \times 2,560$). Images were displayed using a layout of 1×1 on each monitor (size of a displayed image, 33×33 cm), with lung (window level, -700 HU; window width, 1,500 HU) and mediastinal (window level, 40 HU; window width, 400 HU) window settings. The radiologists were not allowed to change the window settings.

Objective image noise

Image noise was defined as the standard deviation of attenuation measured in the air of the tracheal lumen above the aortic arch. CT attenuation was measured in lung and mediastinal window images of ULDCT and RDCT series by one

investigator. The region of interest (ROI) was delineated at the tracheal lumen above the aortic arch, and the size and location of the ROI were kept constant across the four image series. The standard deviation was measured three times, and the mean value was used for analysis.

Subjective visual assessment of image quality

The subjective image quality assessment was performed by two radiologists (YK and SSS; 17 years and 10 years of experience in thoracic CT, respectively) by consensus on a workstation.

Overall image quality

The overall image quality was assessed for various normal pulmonary structures on lung window images using a five-point scale rating system. Radiologists were asked to evaluate five normal lung structures: large central airways including the main bronchi and bronchus intermedius, segmental bronchi and vessels, subsegmental bronchi and vessels, pulmonary vessels in the peripheral 1/3 of the lung, and pleura and subpleural lung. The structures were assessed on a five-point scale (5=excellent image quality without any artefact, 4=slight blurring of the structures that does not restrict image assessment, 3=moderate blurring that slightly restricts assessment, 2=severe blurring causing uncertain evaluation, and 1=non-diagnostic image quality with strong artefacts). Image scores of 4 and 5 were determined to be of diagnostic image quality (Fig. 1).

Before the overall image quality assessment, five training cases including two patients with a BMI > 25 and three with a BMI < 25 were selected among the 81 patients. Their CT images (five sets of ULDCT, five sets of RDCT) were given to the radiologists with their CT parameters and were scored by consensus. For overall image quality assessment, all image sets, from which the patient information and image parameters had been deleted, were assigned numbers in a random order and given to the radiologists for image analysis. To assess the effect of BMI on image quality, the relationship between BMI and image scores was evaluated.

Image quality for various pulmonary lesions

Subjective image quality of pulmonary lesions on ULDCT was compared to that on RDCT. For each patient, radiologists were asked to record any pulmonary lesions and their location on lung window ULDCT images, and then to evaluate the RDCT images. In the next step, ULDCT and RDCT images were aligned next to each other for comparison, and the conspicuity of pulmonary lesions on ULDCT images was assessed with grading as equivalent, superior, or inferior to that on RDCT images. Image quality was also graded as

diagnostic or non-diagnostic for each pulmonary lesion. Image quality was determined as non-diagnostic when pulmonary lesions were not detected or image quality was not sufficient for proper diagnosis on ULDCT at the initial assessment. A maximum of six pulmonary lesions in each patient was included in the analysis.

Pulmonary lesions were categorised as follows: solid nodule (≤ 10 mm in long diameter), ground-glass opacity nodule (≤ 15 mm in long diameter), increased attenuation (ground-glass opacity, consolidation), decreased attenuation (pulmonary emphysema, mosaic attenuation), linear opacity (reticular or linear opacity, interlobular septal thickening), or airway lesions (bronchiectasis, bronchial wall thickening). The lesion location was recorded according to three lung zones (upper, above the carina; middle, between the carina and inferior pulmonary vein; lower, below the inferior pulmonary vein).

Finally, the image quality of calcified lung nodules, calcification of coronary arteries and aorta, and calcification or high attenuation in the mediastinal lymph nodes [8] detected on mediastinal window images were compared between ULDCT and RDCT.

Radiation dose estimations

Radiation dose parameters of CT examinations were assessed from the patient protocol. Volume CT dose index ($CTDI_{vol}$) and dose length product (DLP) were recorded in each patient. Effective radiation dose in mSv was estimated by multiplying the DLP by the chest-specific conversion coefficient (0.014 mSv/mGycm) [9].

Statistical analysis

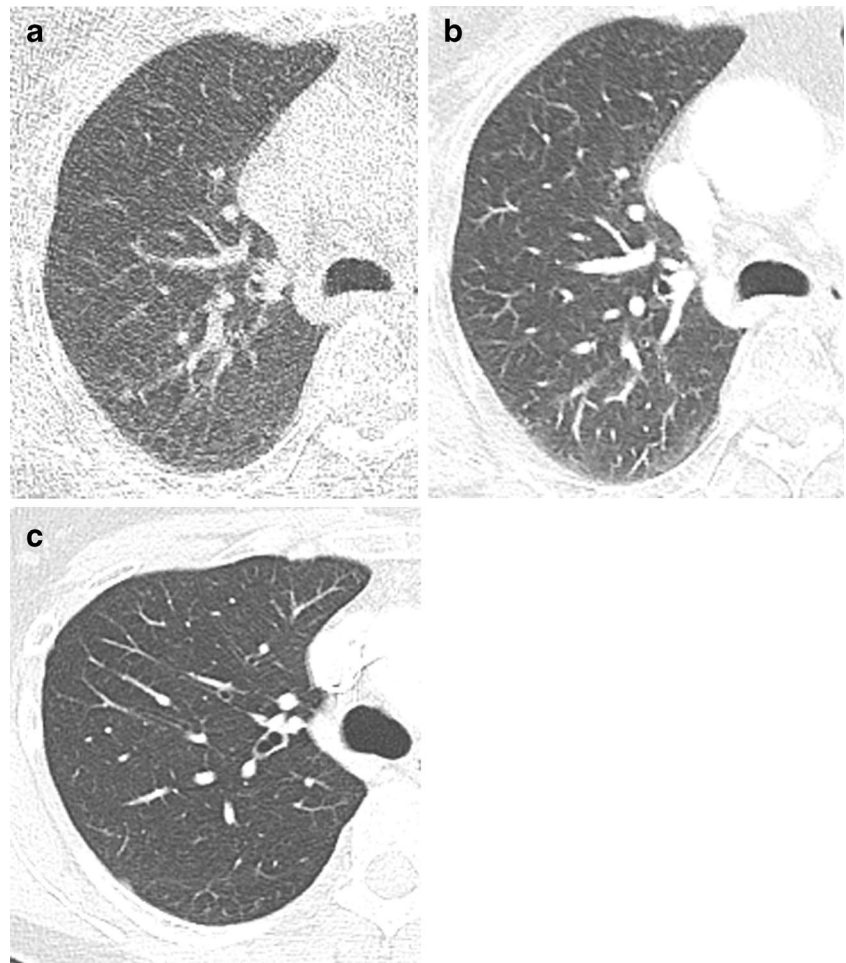
Continuous variables were reported as means \pm standard deviation and categorical variables as frequencies or percentages. The significance of differences in quantitative image quality parameters was tested using paired samples t-tests or the Wilcoxon signed ranks test, depending on the results of the Kolmogorov-Smirnov test. The relationships between BMI and overall image quality scores and between lesion location and ratings of diagnostic image quality were assessed using the Spearman rank order correlation test. All statistical analyses were performed using the SPSS software (SPSS, release 19.0 for Windows; SPSS, Chicago, IL). *P*-values of less than 0.05 were considered to indicate statistical significance.

Results

Image noise

The mean image noise at the tracheal lumen showed significant difference between ULDCT (35.6 ± 12.7 HU at

Fig. 1 Image quality assessment of five normal pulmonary structures on a five-point scale. (a) Image score of 4 (slight blurring of the structures that does not restrict image assessment) for the main bronchi and 3 (moderate blurring of the structures that restricts assessment) for segmental bronchi and vessels, subsegmental bronchi and vessels, pulmonary vessels in the peripheral 1/3 of the lung, and pleura and subpleural lung. (b) Image score for the main bronchi was 5 and that for each of the other four structures was 4. (c) Image score of 5 for all five structures



mediastinal window, 86.7 ± 25.9 HU at lung window) and RDCT (14.5 ± 5.0 HU at mediastinal window, 33.0 ± 7.3 HU at lung window) ($p=0.000$).

Overall image quality of normal structures

The overall image quality scores of ULDCT (19.7 ± 1.2) and RDCT (23.9 ± 1.5) differed significantly ($p < 0.001$). The results of image quality assessment on a five-point scale for normal pulmonary structures are illustrated in Table 1. The image quality of normal lung structures was considered sufficient for reliable diagnosis (i.e., score of 4 or 5) in 91.1 % of ULDCT and 100 % of RDCT images. Significantly more RDCT images were rated as suitable for diagnosis ($p < 0.001$) (Fig. 2).

A significant correlation was observed between the BMI and image score on ULDCT (correlation coefficient, -0.480 ; $p < 0.001$), but not on RDCT (correlation coefficient, -0.141 ; $p = 0.209$) (Fig. 3). The frequency of non-diagnostic image quality (i.e., scores 1–3) was 25.5 % (14/55) in patients with a BMI of 25–30 kg/m^2 and 40.0 % (8/20) with BMI of more than 30 kg/m^2 , while 2.0 % (1/50) with BMI of less than 20 kg/m^2 and 4.6 % (13/280) with BMI of 20–25 kg/m^2 (Table 2).

Image quality for pulmonary lesions

A total of 232 pulmonary lesions from 81 patients were included in the subjective image quality analysis. There were 67 solid nodules (28.9 %) (Fig. 4), 17 ground-glass nodules (7.3 %) (Fig. 5), 57 lesions of increased pulmonary attenuation (24.6 %) (Fig. 6), 23 lesions of decreased pulmonary attenuation (9.9 %) (Fig. 6), 44 lesions of linear opacity (19.0 %) (Fig. 7), and 24 lesions of bronchiectasis or bronchial wall thickening (10.3 %). The mean solid nodule size was 6.9 ± 2.4 mm (range, 3–10 mm) and that of ground-glass nodules was 7.7 ± 2.8 mm (range, 5–13 mm). Lesions were anatomically distributed as follows: 76 lesions (32.8 %) in the upper, 116 lesions (50.0 %) in the middle, and 40 lesions (17.2 %) in the lower lung zone.

Lesion conspicuity on ULDCT was equal to that on RDCT in 152 lesions (65.5 %) and inferior in 80 lesions (34.5 %), and image quality on ULDCT was diagnostic for 206 lesions (88.8 %) and non-diagnostic for 26 lesions (11.2 %) (Table 3).

Lesion conspicuity and diagnostic image quality according to location are summarised in Table 2. Non-diagnostic image quality was observed in 2 (3.0 %) solid nodules, 4 (23.5 %)

Table 1 Subjective assessment of image quality for normal pulmonary structures

	ULDCT			RDCT	
	Image score ¹				
Normal pulmonary structures	3	4	5	4	5
Large central airways	0 ²	74 (91.4)	7 (8.6)	4 (4.9)	77 (95.1)
Segmental bronchi and vessels	2 (2.5)	75 (92.6)	4 (4.9)	18 (22.2)	63 (77.8)
Subsegmental bronchi and vessels	6 (7.4)	74 (91.4)	1 (1.2)	33 (40.7)	48 (59.3)
Peripheral 1/3 pulmonary vessels	17 (21.0)	63 (77.8)	1 (1.2)	27 (33.3)	54 (59.3)
Pleura and subpleural lung	11 (13.6)	68 (84.0)	2 (1.2)	10 (12.3)	71 (87.7)
Total	36 (8.9)	354 (87.4)	15 (3.7)	92 (22.7)	313 (77.3)

¹ Image score: 5=excellent image quality without any artefact; 4=slight blurring of the structures that does not restrict image assessment; 3=moderate blurring that slightly restricts assessment; 2=severe blurring causing uncertain evaluation; 1=non-diagnostic image quality with strong artefacts. Image scores of 4 and 5 were determined to be of diagnostic quality.

² Numbers are frequencies of images (five per patient; total number of patients, 81) with percentages in parentheses.

ULDCT, ultra low-dose CT; RDCT, reduced-dose CT

ground-glass nodules, 2 lesions (3.5 %) of increased attenuation, 14 lesions (60.9 %) of decreased attenuation, 3 lesions (6.8 %) of linear opacity, and 1 lesion (4.2 %) of bronchiectasis or bronchitis.

Among 14 decreased-attenuation lesions of non-diagnostic image quality, six were mild to severe pulmonary emphysema located in the upper lung zone that were severely affected by beam-hardening artefacts at shoulder joints, and eight were mosaic attenuation in upper or middle lung zones (Fig. 6). One of two solid nodules was small (3 mm) and located in the apex, and the other nodule in the middle lung zone, noted in a patient with relatively high BMI (27.4 kg/m²) (Fig. 4d), was also small (4 mm). Four ground-glass nodules had lower attenuation than other ground-glass nodules and two were small in size (4 mm) (Fig. 5d). Two increased

attenuation lesions were small ill-defined ground-glass opacity lesions located in the upper lobe or subpleural dependent area of the lower lobe, and affected by beam hardening by the shoulders and ribs. Three linear opacity lesions and a focal bronchiectasis were located at the apex; two were noted in patients with a high BMI (>25 kg/m²).

In a correlation analysis, no significant relationship was noted between lesion location and diagnostic image quality for any category of pulmonary lesions except lesions of decreased attenuation. For these lesions, including pulmonary emphysema and mosaic attenuation, non-diagnostic image quality was more frequent in the upper lung zones (correlation coefficient, -0.501 ; $p=0.015$).

In mediastinal window images, calcifications in lung nodules, coronary arteries, aorta, and lymph nodes

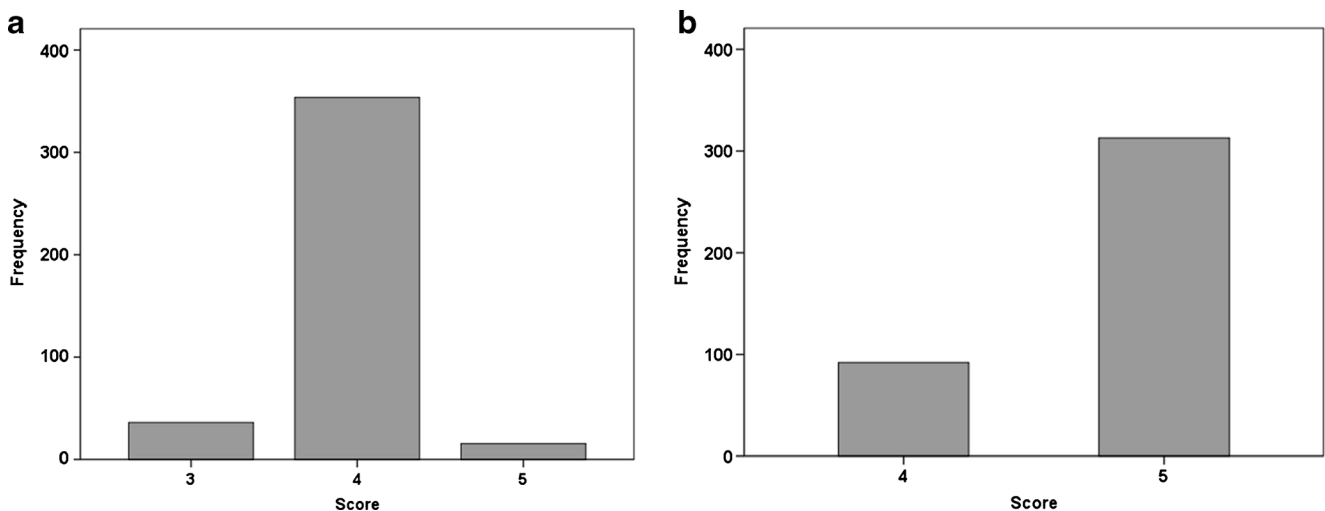


Fig. 2 Subjective image scores of various lung structures on ultra-low-dose CT (ULDCT) (a) and reduced-dose CT (RDCT) (b). Overall, 91.1 % of ULDCT and 100 % of RDCT images were considered of diagnostic quality (i.e., score of 4 or 5)

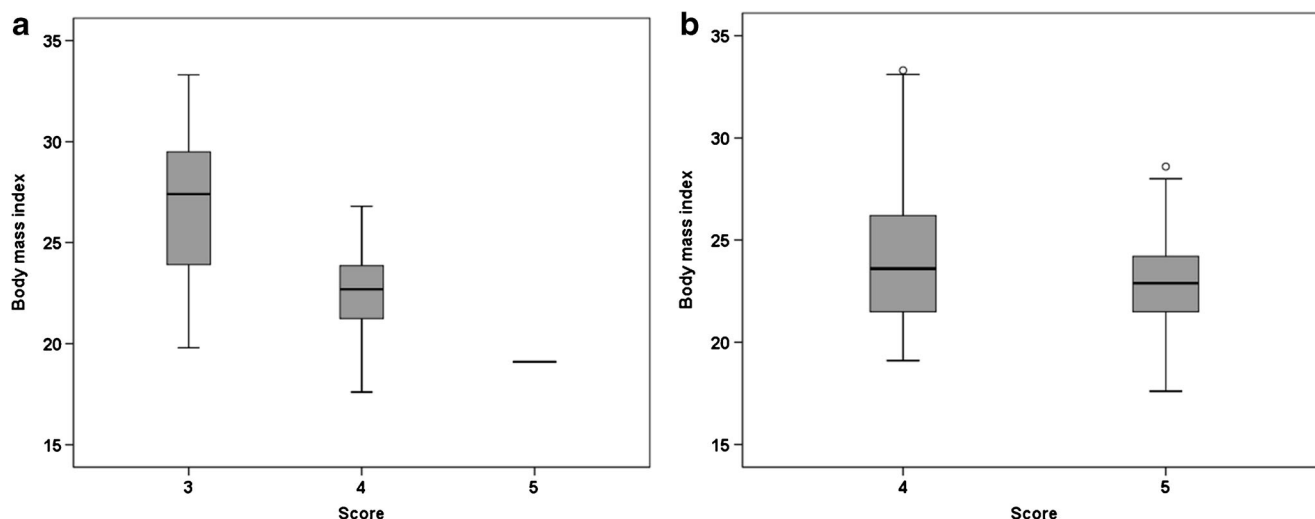


Fig. 3 Relationship between body mass index (BMI) and subjective image scores of various lung structures on ultra-low-dose CT (ULDCT) (a) and reduced-dose CT (RDCT) (b). Non-diagnostic image quality (i.e., score ≤ 3) on ULDCT was more frequent in the groups of patients with a BMI > 25 kg/m²; 2.0 (1/50), 4.6 (13/280), 25.5 (14/55), and 40.0 (8/20)%

for BMIs of < 20 , 20–25, 25–30, and > 30 , respectively. A significant correlation was observed between the BMI and image score on ULDCT (correlation coefficient, -0.480 ; $p < 0.001$), but not on RDCT (correlation coefficient, -0.141 ; $p = 0.209$)

appeared slightly larger on ULDCT than on RDCT, and some small coronary artery calcifications were noted only on ULDCT. Detection of high attenuation in lymph nodes, where attenuation is greater than in the great vessels, on ULDCT was an informative supplement to contrast-enhanced RDCT in which intrinsic high attenuation of lymph nodes was not discriminated from contrast enhancement.

Radiation dose

The mean CTDI_{vol}, DLP, and effective radiation dose were 0.61 ± 0.0 mGy (range, 0.60–0.61 mGy), 20.8 ± 2.0 mGy·cm (range, 16–25 mGy·cm), and 0.29 ± 0.03 mSv (0.22–0.35 mSv), respectively, for the ULDCT protocol and 5.5 ± 2.1 mGy (range, 2.3–13.5 mGy), 204.1 ± 78.1 mGy·cm (range, 109–490 mGy·cm), and 2.88 ± 1.11 mSv (1.53–6.86 mSv), respectively, for the RDCT protocol.

Table 2 Distribution of non-diagnostic image quality on ultra-low-dose CT according to body mass index (BMI)

BMI (kg/m ²)	Number of patients ($n=33$)	Frequency of non-diagnostic image quality ¹
≤ 20	10	1/50 (2.0 %)
$20 <, \leq 25$	56	13/280 (4.6 %)
$25 <, \leq 30$	11	14/55 (25.5 %)
$30 <$	4	8/20 (40.0 %)
Total	81	36/405 (8.9 %)

¹ Proportion of images (five per patient) of various pulmonary structures assigned scores < 3 on a 1–5 scale

Discussion

Recent increases in the diagnostic accuracy of CT following the introduction of helical or multidetector CT have greatly increased the variety of clinical indications for CT. In screening for lung cancer or the diagnosis of benign lung parenchymal diseases such as pulmonary infection, CT is usually performed without contrast enhancement and using a low radiation dose. Although the low-dose CT currently used involves lower radiation exposure than conventional CT, the radiation dose is still a concern in young patients and those undergoing repetitive CT examinations, such as patients undergoing lung cancer screening.

Various types of iterative reconstruction algorithms have recently been introduced to reduce the radiation dose from CT. Iterative reconstruction, an alternative to the conventional filtered back-projection (FBP) algorithm, can reduce the radiation dose by repeated subtraction of quantum noise, eliminating artefacts [6]. Sinogram-affirmed iterative reconstruction (SAFIRE), applied in the current study, uses a noise-modelling technique supported by raw data, in which the model utilises the known propagation of noise in projection data into the image domain and the noise content is then subtracted in each iteration. The resulting noise-subtracted image is compared with the initial data to generate an updated image, which is added to the previous data set before the next iteration [10].

Many studies have reported that iterative reconstruction may preserve or improve the image quality of unenhanced chest CT obtained with a reduced radiation dose [11–18]. We demonstrated in our study that SAFIRE yields diagnostic image quality in 87 % of non-enhanced chest CT images of

Fig. 4 Image quality of solid nodules. A 3-mm solid nodule in a 74-year-old man with a BMI of 19.1 kg/m^2 was diagnosed on both RDCT (a) and ULDCT (b). Image quality of a 3-mm nodule in a 72-year-old man with a BMI of 27.4 kg/m^2 was diagnostic on RDCT (c), but non-diagnostic on ULDCT (d)

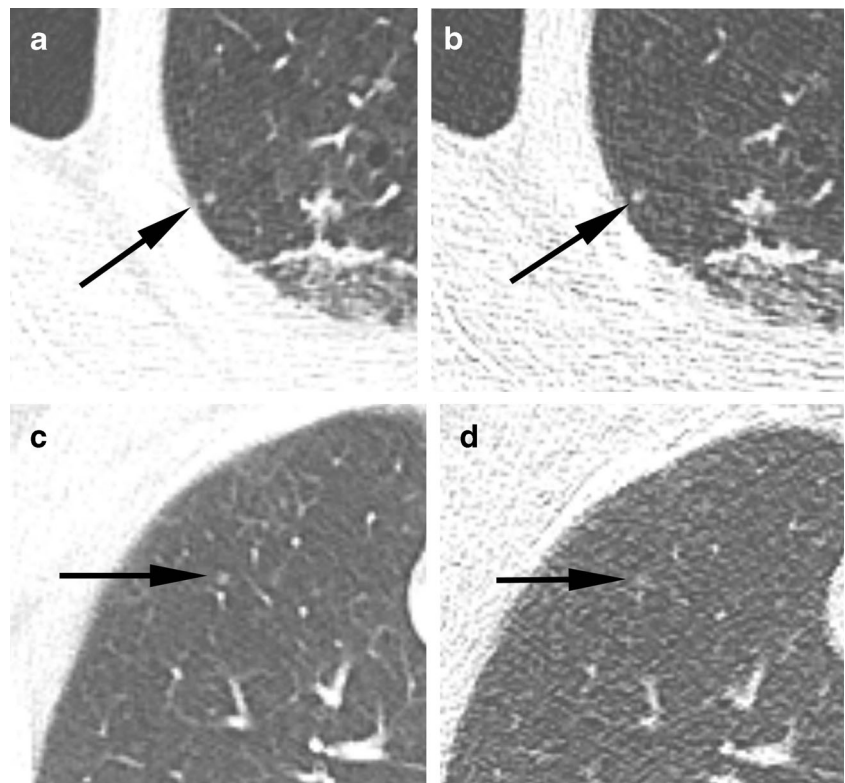


Fig. 5 Ground-glass opacity nodules. An 8-mm ground-glass opacity nodule in a 68-year-old woman with a BMI of 30.0 kg/m^2 was diagnosed on both RDCT (a) and ULDCT (b). Image quality of an 8-mm faint ground-glass opacity nodule in an 81-year-old man with a BMI of 24.7 kg/m^2 was diagnostic on RDCT (c), but non-diagnostic on ULDCT (d)

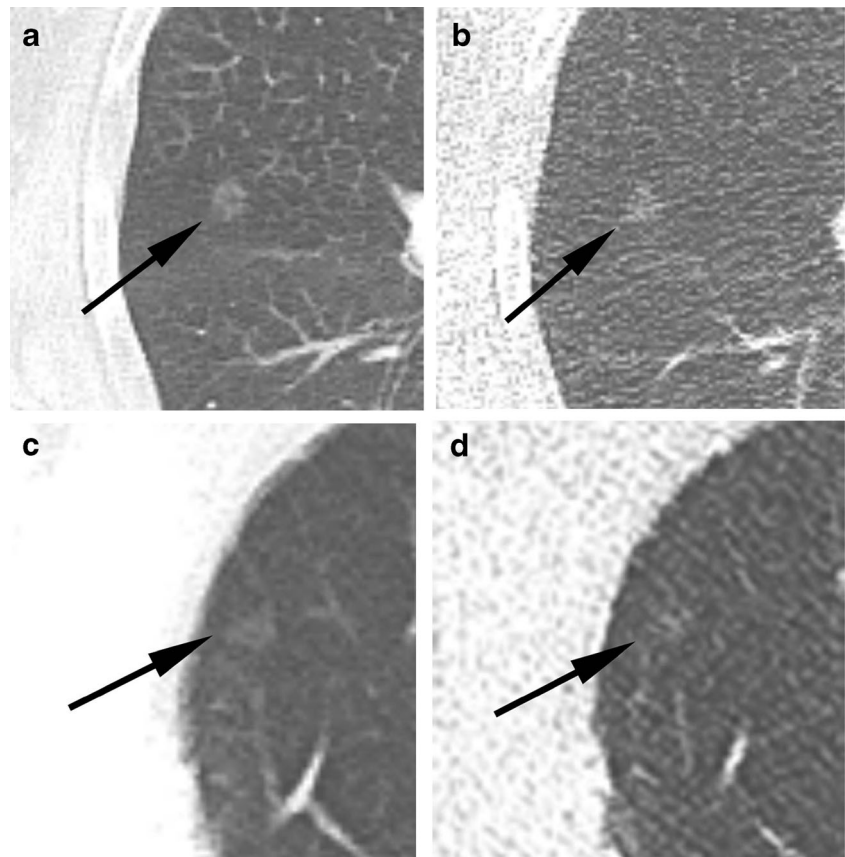
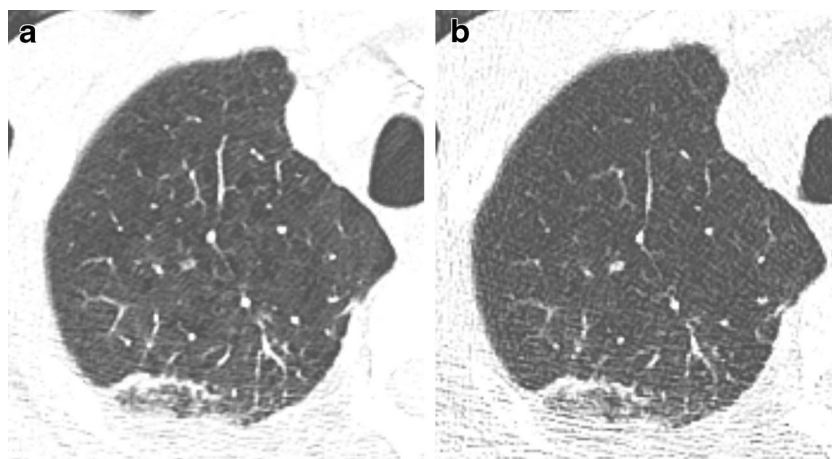


Fig. 6 In a 74-year-old man with a BMI of 19.1 kg/m^2 centrilobular pulmonary emphysema visible on RDCT (a) was not diagnosed on ULDCT (b). Consolidation was well visualised on both RDCT and ULDCT



normal anatomic structures and 89 % of abnormal pulmonary lesions at 0.3 mSv. These results are lower than those of a previous report of low-dose CT using SAFIRE at 0.5 mSv in which diagnostic image quality was obtained in 98 % of patients [6]. However, in patients with a BMI of less than 25 kg/m^2 , our study also found that this reconstruction algorithm produced images of diagnostic quality in more than 95 % of cases, while in patients with a BMI $>25 \text{ kg/m}^2$, the rate was decreased substantially to $\sim 70 \%$.

In the current study, we also evaluated the acceptability of this ultra-low-radiation dose CT method for the assessment of various pulmonary lesions. ULDCT yielded diagnostic image quality for 93–97 % of each type of pulmonary lesion, except decreased-attenuation lesions (emphysema and air trapping) or ground-glass opacity nodules. Only 60 % of decreased-attenuation lesions were diagnosed, and most non-diagnosable lesions were located in the upper or sometimes middle lung zones, which are more affected by beam hardening due to the bony structures of the shoulder than the lower lung zone. For ground-glass opacity nodules, low attenuation and small size ($\leq 4 \text{ mm}$) rather than lesion location were the main causes of non-diagnostic image quality.

Previous studies have shown that a reduced radiation dose can be used for CT examinations to assess abnormalities that

present a high contrast to normal lung areas, such as pulmonary nodules or consolidations [15,19–21]. In our study, 96–97 % of consolidation, solid nodules, or bronchial diseases were diagnosed on ULDCT.

According to our results, image quality resulting from very-low-radiation-dose CT depends not only on the patient body type but also on the type of pulmonary lesions. Therefore, the ULDCT parameters in the current study (80 kVp and 30 mAs; effective radiation dose, 0.3 mSv; iterative reconstruction) may be used for the evaluation of pneumonia, bronchiectasis, or solid nodules $>4 \text{ mm}$ in patients with BMI $<25 \text{ kg/m}^2$. However, in obese patients or when evaluating pulmonary emphysema or ground-glass opacity nodules, ULDCT should be performed with higher radiation doses.

In our study, ULDCT was performed prior to contrast enhancement and provided information not visualised on post-enhanced CT images, including calcification of vascular structures and lymph nodes. Better visualisation of calcification by ULDCT likely results from both lack of contrast enhancement and the fact that lowering the tube potential in CT provides higher attenuation of calcification as a result of the greater photoelectric effect.

In our study, the effective radiation dose was 0.3 mSv, which is much lower than that of standard low-dose CT scans

Fig. 7 Interlobular septal thickenings (arrows) and consolidation are well visualised on both RDCT (a) and ULDCT (b)

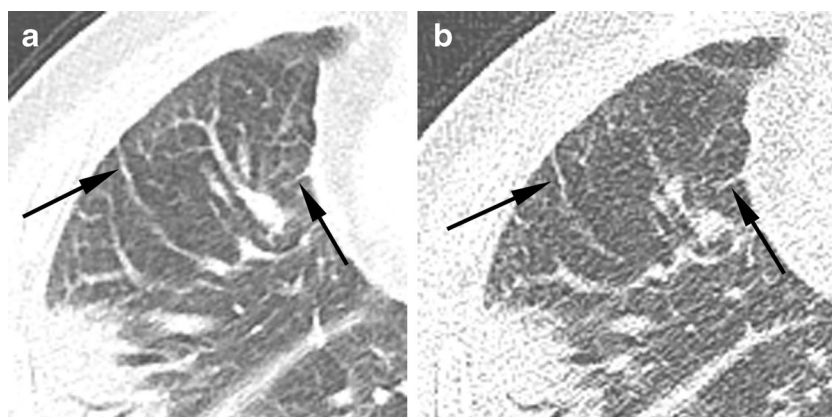


Table 3 Subjective assessment of image quality for various pulmonary lesions

Lesion	Lesion location	No. of lesions	Lesion conspicuity on ULDCT compared to RDCT ¹		Image quality for diagnosis on ULDCT	
			Inferior	Equal	D	ND
Solid nodule (≤ 10 mm)	Upper	13	2	13	12	1
	Middle	39	5	34	38	1
	Lower	15	2	13	15	0
		67	9 (13.4 %)	58 (86.6 %)	65 (97.0 %)	2 (3.0 %)
Ground-glass nodule (≤ 15 mm)	Upper	3	0	3	3	0
	Middle	12	7	5	8	4
	Lower	2	0	2	2	0
		17	7 (41.2 %)	10 (58.8 %)	13 (76.5 %)	4 (23.5 %)
Increased attenuation	Upper	19	11	8	18	1
	Middle	29	13	16	29	0
	Lower	9	4	5	8	1
		57	28 (49.1 %)	29 (50.9 %)	55 (96.5 %)	2 (3.5 %)
Decreased attenuation	Upper	11	10	1	2	9 ²
	Middle	9	8	1	4	5 ²
	Lower	3	3	0	3	0 ²
		23	21 (91.3 %)	2 (8.7 %)	9 (39.1 %)	14 (60.9 %)
Linear opacities	Upper	21	5	16	18	3
	Middle	18	6	12	18	0
	Lower	5	0	5	5	0
		33	11 (25.0 %)	33 (75.0 %)	41 (93.2 %)	3 (6.8 %)
Bronchiectasis or bronchitis	Upper	9	3	6	8	1
	Middle	9	1	8	9	0
	Lower	6	0	6	6	0
		24	4 (16.7 %)	20 (86.3 %)	23 (95.8 %)	1 (4.2 %)
Total		232 (100 %)	80 (34.5 %)	152 (65.5 %)	206 (88.8 %)	26 (11.2 %)

¹ No lesions had superior lesion conspicuity on ULDCT compared to RDCT.

² Significant correlation between lesion location and proportion of images of diagnostic quality (correlation coefficient, -0.501 ; $p=0.015$).

ULDCT, ultra low-dose CT; RDCT, reduced-dose CT; D, diagnostic; ND, non-diagnostic

(0.8–1.5 mSv) [22,23] and similar to that of posterior-anterior and lateral chest radiographs. We did not use automated tube current modulation since the relatively high attenuation at the level of the shoulders necessitated a high tube current, resulting in greater radiation exposure.

The current study had several limitations. First, for the assessment of subjective image quality, RDCT images rather than standard dose CT were used as reference standards. However, the diagnostic performance of RDCT using automated tube potential selection and dose modulation has been confirmed to be comparable to standard-dose CT. Gnannt et al. found no significant difference in subjective image quality between CT using automated tube potential selection (mean $CTDI_{vol}$, 8.6 ± 2.8 mGy) and 120 kVp fixed tube potential (9.8 ± 1.8 mGy), although the mean image score was slightly higher for fixed tube potential CT [24]. Second,

motion artefacts may differ between ULDCT and RDCT because they were not performed simultaneously. RDCT was performed following ULDCT within a short time interval. Third, this study was performed in a small population, and only four of our patients had a BMI > 30 kg/m². Further studies in larger patient populations with more diverse body types are required to confirm these preliminary findings. Fourth, the comparison was performed between non-contrast-enhanced ULDCT and contrast-enhanced RDCT. Contrast enhancement may influence the overall image quality; therefore, we compared only lung window images that appeared minimally influenced by contrast enhancement.

In conclusion, ULDCT using iterative reconstruction (SAFIRE) at 80 kVp with an effective dose of 0.3 mSv generates images of diagnostic quality in patients with BMIs

≤25, but is of limited use for lesions with decreased attenuation, ground-glass nodules, or located in the upper lobe.

Acknowledgements The scientific guarantor of this publication is Yookyung Kim. The authors of this manuscript declare no relationships with any companies whose products or services are related to the subject matter of the article. The authors state that this work has not received any funding. No complex statistical methods were necessary for this article. Institutional Review Board approval was obtained. Written informed consent was waived by the Institutional Review Board. Methodology: retrospective, observational, performed at one institution

References

- Kalra MK, Maher MM, Toth TL et al (2004) Strategies for CT radiation dose optimization. *Radiology* 230:619–628. doi:10.1148/radiol.2303021726
- Qi W, Li J, Du X (2009) Method for automatic tube current selection for obtaining a consistent image quality and dose optimization in a cardiac multidetector CT. *Korean J Radiol* 10:568–574. doi:10.3348/kjr.2009.10.6.568
- Heyer CM, Mohr PS, Lemburg SP, Peters SA, Nicolas V (2007) Image quality and radiation exposure at pulmonary CT angiography with 100- or 120-kVp protocol: Prospective randomized study. *Radiology* 245:577–583. doi:10.1148/radiol.2452061919
- Loeve M, Lequin MH, de Bruijne M et al (2009) Cystic fibrosis: Are volumetric ultra-low-dose expiratory CT scans sufficient for monitoring related lung disease? *Radiology* 253:223–229. doi:10.1148/radiol.2532090306
- Hwang HJ, Seo JB, Lee JS et al (2012) Radiation dose reduction of chest CT with iterative reconstruction in image space - part I: Studies on image quality using dual source CT. *Korean J Radiol* 13:711–719. doi:10.3348/kjr.2012.13.6.711
- Baumueeller S, Winklehner A, Karlo C et al (2012) Low-dose CT of the lung: Potential value of iterative reconstructions. *Eur Radiol* 22:2597–2606. doi:10.1007/s00330-012-2524-0
- Silva AC, Lawder HJ, Hara A, Kujak J, Pavlicek W (2010) Innovations in CT dose reduction strategy: Application of the adaptive statistical iterative reconstruction algorithm. *AJR Am J Roentgenol* 194:191–199. doi:10.2214/AJR.09.2953
- Yoo SY, Kim Y, Cho HH et al (2013) Dual-energy CT in the assessment of mediastinal lymph nodes: Comparative study of virtual non-contrast and true non-contrast images. *Korean J Radiol* 14:532–539. doi:10.3348/kjr.2013.14.3.532
- AAPM (2008) AAPM report no. 96: The measurement, reporting, and management of radiation dose in CT. College Park: American Association of Physicists in Medicine.
- Moscariello A, Takx RA, Schoepf UJ et al (2011) Coronary CT angiography: Image quality, diagnostic accuracy, and potential for radiation dose reduction using a novel iterative image reconstruction technique-comparison with traditional filtered back projection. *Eur Radiol* 21:2130–2138. doi:10.1007/s00330-011-2164-9
- Hu XH, Ding XF, Wu RZ, Zhang MM (2011) Radiation dose of non-enhanced chest CT can be reduced 40 % by using iterative reconstruction in image space. *Clin Radiol* 66:1023–1029. doi:10.1016/j.crad.2011.04.008
- Mets OM, Willeminck MJ, de Kort FP et al (2012) The effect of iterative reconstruction on computed tomography assessment of emphysema, air trapping and airway dimensions. *Eur Radiol* 22:2103–2109. doi:10.1007/s00330-012-2489-z
- Prakash P, Kalra MK, Ackman JB et al (2010) Diffuse lung disease: CT of the chest with adaptive statistical iterative reconstruction technique. *Radiology* 256:261–269. doi:10.1148/radiol.10091487
- Singh S, Kalra MK, Gilman MD et al (2011) Adaptive statistical iterative reconstruction technique for radiation dose reduction in chest CT: A pilot study. *Radiology* 259:565–573. doi:10.1148/radiol.11101450
- Neroladaki A, Botsikas D, Boudabbous S, Becker CD, Montet X (2013) Computed tomography of the chest with model-based iterative reconstruction using a radiation exposure similar to chest X-ray examination: Preliminary observations. *Eur Radiol* 23:360–366. doi:10.1007/s00330-012-2627-7
- Qi LP, Li Y, Tang L et al (2012) Evaluation of dose reduction and image quality in chest CT using adaptive statistical iterative reconstruction with the same group of patients. *Br J Radiol* 85:e906–11. doi:10.1259/bjr/66327067
- Yamada Y, Jinzaki M, Hosokawa T et al (2012) Dose reduction in chest CT: Comparison of the adaptive iterative dose reduction 3D, adaptive iterative dose reduction, and filtered back projection reconstruction techniques. *Eur J Radiol* 81:4185–4195. doi:10.1016/j.ejrad.2012.07.013
- Pontana F, Pagniez J, Flohr T et al (2011) Chest computed tomography using iterative reconstruction vs filtered back projection (part 1): Evaluation of image noise reduction in 32 patients. *Eur Radiol* 21:627–635. doi:10.1007/s00330-010-1990-5
- Bankier AA, Schaefer-Prokop C, De Maertelaer V et al (2007) Air trapping: Comparison of standard-dose and simulated low-dose thin-section CT techniques. *Radiology* 242:898–906. doi:10.1148/radiol.2423060196
- Karabulut N, Toru M, Gelebek V, Gulsun M, Ariyurek OM (2002) Comparison of low-dose and standard-dose helical CT in the evaluation of pulmonary nodules. *Eur Radiol* 12:2764–2769. doi:10.1007/s00330-002-1368-4
- Weng MJ, Wu MT, Pan HB, Kan YY, Yang CF (2004) The feasibility of low-dose CT for pulmonary metastasis in patients with primary gynecologic malignancy. *Clin Imaging* 28:408–414. doi:10.1016/S0899-7071(03)00246-8
- Baldwin DR, Duffy SW, Wald NJ, Page R, Hansell DM, Field JK (2011) UK lung screen (UKLS) nodule management protocol: Modelling of a single screen randomised controlled trial of low-dose CT screening for lung cancer. *Thorax* 66:308–313. doi:10.1136/thx.2010.152066
- National Lung Screening Trial Research Team, Aberle DR, Berg CD et al (2011) The national lung screening trial: Overview and study design. *Radiology* 258:243–253. doi:10.1148/radiol.10091808
- Gnannt R, Winklehner A, Eberli D, Knuth A, Frauenfelder T, Alkadhi H (2012) Automated tube potential selection for standard chest and abdominal CT in follow-up patients with testicular cancer: Comparison with fixed tube potential. *Eur Radiol* 22:1937–1945. doi:10.1007/s00330-012-2453-y